Tunable double-cavity solid-spaced bandpass filter

Johan Floriot, Fabien Lemarchand and Michel Lequime

Institut Fresnel – UMR CNRS 6133
Université Paul Cézanne – Domaine Universitaire de Saint-Jérôme
13397 Marseille Cedex 20, France
johan.floriot@fresnel.fr

Abstract: In this paper, we introduce the principle and demonstrate the feasibility of a tunable multiple-cavity solid-spaced bandpass filter for WDM (Wavelength Division Multiplexing) applications, which uses a vernier effect since the two cavities have different thermal sensitivities. A set of specific wavelengths can be addressed in the whole C-Band by using temperature changes less than 100°C. This result corresponds to a gain factor in sensitivity about 5 with respect to alternative standard thin-film configurations.

OCIS codes: (060.4510) Optical Communications, (060.1810) Multiplexing, (230.5750) Resonators, (350.2460) Filters, Interference, (310.6860) Thin Films, (160.6840) Thermo-Optical Materials

References and links

1. J. Floriot, F. Lemarchand and M. Lequime, "Double coherent solid-spaced filters for very narrow-bandpass filtering applications," Opt. Commun. **222**, 101-106 (2003).
2. J. Floriot, F. Lemarchand and M. Lequime, "Cascaded solid-spaced filters for DWDM applications," in Advances in Optical Thin-Films, C. Amra, N. Kaiser and H.A. Macleod, eds., Proc. SPIE **5250**, 384-392 (2003).
3. J. Floriot, F. Lemarchand and M. Lequime, "Solid-spaced filters: an alternative for narrow bandpass applications," in Proceedings of Optical Interference Coatings, Tucson (2004).
4. J.A. Dobrowolski, "Mica interference filters with transmission bands of very narrow half-widths," J. Opt. Soc. Am. **49**, 794-806 (1959).
5. R.R. Austin, "The use of solid etalon devices as narrowband interference filters," Opt. Eng. **11**, 68-69 (1972).
6. M. Candille and J.M. Saurel, "Réalisation de filtres double onde à bandes passantes très étroites sur supports en matière plastique (mylar)," Opt. Acta **21**, 947-962 (1974).
7. S.D. Smith and C.R. Pidgeon, "Application of multiple beam interferometric methods to the study of CO_2 emission at 15 µm," mém. Soc. R. Sci. Liège 5è série 9, 336-349 (1963).
8. A.E. Roche and A.M. Title, "Tilt tunable ultra narrow-band filters for high resolution photometry," Appl. Opt. **14**, 765-770 (1974).
9. L. Domash, E. Ma, N. Nemchuk, A. Payne and M. Wu, "Tunable thin-film filters based on thermo-optic semiconductor films," in Applications of Photonic Technology V, R. A. Lessard, G. A. Lampropoulos and G. W. Schinn, eds., Proc. SPIE **4833**, 685-695 (2002).
10. L. Domash, M. Wu, N. Nemchuck and E. Ma, "Tunable and Switchable Multiple-Cavity Thin Film Filters," J. Lightwave Technol. **22**, 126-135 (2004).
11. L. Domash, M. Wu, N. Nemchuk and R. Murano, "Switchable thin film add/drop filter," presented at the Optical Fiber Conf., Optical Soc. America, Atlanta, GA (2003).
12. W. Gunning, "Double-cavity electrooptic Fabry-Perot tunable filter," Appl. Opt. **17**, 3129-3131 (1982).
13. M. Lequime, R. Parmentier, F. Lemarchand and C. Amra, "Towards tunable thin film filters for WDM applications," Appl. Opt. **41**, 3277-3284 (2002).
14. M. Bass, E. van Stryland, D. Williams and W. Wolfe, *Handbook of Optics* (McGraw-Hill Professional, 2nd edition, 1994).
15. J. Haisma, B. Spierings, U. Bierman and A. Van Gorkum, "Diversity and feasibility of direct bonding: a survey of a dedicated optical technology," Appl. Opt. **33**, 1154-1169 (1994).
16. A. Plössl and G. Kraüter, "Wafer direct bonding: tailoring adhesion between brittle materials," Mat. Sci. and Eng. R**25**, 1-88 (1999).

17. J. Floriot, F. Lemarchand and M. Lequime are preparing a manuscript to be called "High accuracy measurement of the residual air gap thickness of thin-film and solid-spaced filters assembled by optical contacting."

1. Introduction

The fabrication of very narrow bandpass filters with high rejection level (less than -25dB) and very sharp spectral response answers to crucial needs in optical telecommunications. These filters allow to insert or extract (ADD/DROP) a particular wavelength (or channel) from the ITU (International Telecommunication Union) grid; they are also used to separate (demultiplexing) or to group (multiplexing) several channels at both sides of an optical line. We have proposed in recent papers [1-3] an alternative solution to design such filters. This approach, already studied during past decades for different applications [4-8], is based on the use of thick cavities (in the range of 100µm) with high optical quality (in terms of homogeneity, transparency, roughness and parallelism). We demonstrated that it is possible to fabricate high-finesse-Fabry-Perot filters with WDM (Wavelength Division Multiplexing) performances by depositing broad-band dielectric mirrors on both sides of silica thick cavities. Simple, double and triple cavity filters with (ADD/DROP [1-3]) or without (interleaver [3]) autofiltering properties were achieved by this method. All theses studies deal only with passive structures which present no tunability.

On the other hand, one of the advantages of thick cavities is that we can select active and/or crystalline materials for them and also achieve spectral tunability by applying an external command. Such a property will help to answer the increasing demand for network flexibility and cost reduction. Different effects can lead to a modification of the optical thickness *nd* of the cavities (variation of the refractive index *n* and/or variation of the mechanical thickness *d*) and therefore to a spectral shift of the filter response. Electro-optic effects in lithium niobate are small and lead to shifts of about 0.1nm for an electric field near the damage threshold (10^7V/m). Thermal effects in silicon are much more interesting because of the high value of the thermo-optic coefficient of this material. Domash and al. proposed to use multiple-cavity-thin-film filters with cavities made of hydrogenated amorphous silicon a:Si-H and thus achieved center wavelength sensitivities around 100pm/°C [9,10]. However, it means that 400°C temperature variations are required to achieve a tunability across the whole C-Band (1530 - 1570 nm). To transform tunable filters into optical switches [10,11], Domash and al. proposed also to join one active a:Si-H thin-film cavity and four passive silica thin-film cavities. The active cavity is designed to be matched with the passive one at a given temperature and the transmission of the optical switch is then close to 100% at the design wavelength. When the temperature increases, this matching progressively disappears because of the large difference in the thermal sensitivities of both materials and the filter assembly becomes totally reflective. We propose to transpose this last scheme to a solid-spaced double-cavity bandpass filter in order to obtain, by a temperature change, not only a mismatching of both cavities at the design wavelength but also their matching at a new wavelength: we can talk of discrete tuning, at the opposite of the continuous tuning corresponding to the first scheme used by Domash. This vernier effect approach has been studied in the case of $LiNbO_3$ cavities near 3.5µm. But, in this case the filter is polarization-dependent, the transmittance is only of a few percent and the applied electric field stays near the damage threshold [12].

We will describe, in the following sections of this paper, the principle of this discrete tuning, the experimental results which demonstrate clearly the feasibility of such a filter and the guidelines of a method for designing double-cavity tunable filters whose central wavelength can be thermally switched from a given channel of the ITU grid to another one, 8 or 16 channels apart.

2. Principle of the method

We present first a description of the vernier effect on a tandem solid-spaced two-cavity filter that will be studied experimentally in the next part. Let us consider a silica cavity with an optical thickness of $376\lambda_0/4$ and a silicon one with an optical thickness of $536\lambda_0/4$ (λ_0=1550nm) coated on both sides with dielectric mirrors. The refractive indexes of the cavities are respectively 1.444 and 3.477 at 1550nm. The spectral shift of each solid-spaced cavity is defined by [13]:

$$\frac{\Delta\lambda}{\lambda_0} = \kappa \frac{\Delta(nd)}{nd} \quad \text{where} \quad \kappa = \frac{1}{1 - \dfrac{\lambda_0}{2k\pi} \cdot \dfrac{\partial\varphi}{\partial\lambda}} \tag{1}$$

where k is the interference order and $\partial\varphi/\partial\lambda$ the reflective phase dispersion of the mirrors. As soon as thick cavities are considered, k is over 100, so that $\kappa \approx 1$. Then, the thermal sensitivity of the filter only depends on the nature of the spacer. By using thermal data [14] of respectively fused silica $(1/nd).[\partial(nd)/\partial T] \approx 7.8\ 10^{-6}$/K] and bulk silicon $[(1/nd).[\partial(nd)/\partial T] \approx 5.1\ 10^{-5}$/K], we can compute the thermal shift of the center wavelength of each solid-spaced filter, which is respectively equal to 12pm/°C for the silica one and 95pm/°C for the silicon one. For 0.4nm-FWHM (Full Width at Half Maximum) filters, we must consider 5-layer-dielectric-mirrors on silica cavity and 4-layer-dielectric-mirrors on silicon cavity (the mirrors are made of silica and tantalum pentoxide whose indexes are respectively 1.46 and 2.09 at 1550nm). Figure 1 is a small movie that shows the transmission spectra of each filter between 1520 and 1570nm when the temperature is increased by 5°C steps. Initially (T = 25°C), the filters are in coincidence at 1550nm. When the temperature progressively increases, the initial coincidence tends to disappear and another one appears around 1534nm. This first jump takes place when the temperature variation ΔT is about 14°C. When increasing again the temperature, others coincidences successively appear around 1559nm (for ΔT = 36°C), 1542.5nm (for ΔT = 50°C), and so on.

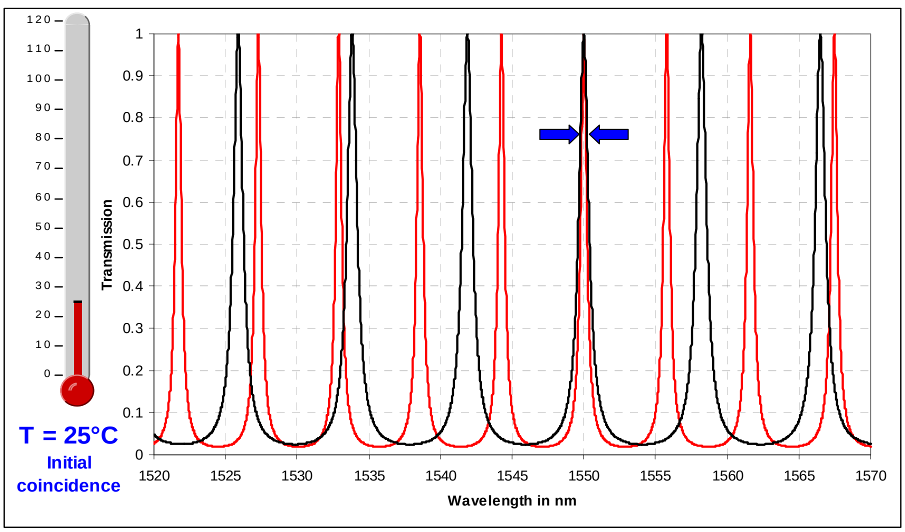

Fig. 1. (1.63 MB) Movie of the thermal dependence of both filter transmission (black: silica; red: silicon).

Table 1 recapitulates these results. The third column represents the successive shifts and the fourth column the differential sensitivity, i.e. the ratio between these spectral shifts and the temperature changes needed to switch from a wavelength to the following.

Table 1. Theoretical coincidences and related sensitivities

ΔT (°C)	*Center wavelength (nm)*	*Spectral shift (nm)*	*Differential sensitivity (pm/°C)*
0	1550.00	0	
14	1533.99	-16.0	-1143
36.5	1558.67	24.7	+1098
50	1542.45	-16.2	-1200
64	1526.63	-15.8	-1129
73	1567.39	40.8	+1143
86	1551.01	-16.4	-1261

We shall stress that the behaviour of the system is pseudo-periodic: for ΔT = 86°C, the coincidence is indeed nearly at the same location as the initial one. Nevertheless, a residual deviation (1nm) exists at the end of each cycle because of the silica intrinsic thermal dependence. This deviation can be used to address a different set of wavelengths for each consecutive cycle.

The differential sensitivity is quasi-constant between two successive coincidences; its average absolute value is 1162pm/°C, about 12 times higher than the sensitivity of silicon. Figure 2 shows the transmission window of the resulting double-cavity filter and Fig. 3 shows this transmission spectrum over the band (1520-1570nm) at T = 25°C (ΔT = 0°C) when both filters are coherently cascaded, using a quarter-wavelength air gap as the coupling layer.

Since thermal effects are considered, the response time of the filter may be relatively long, in the several tens of milliseconds range.

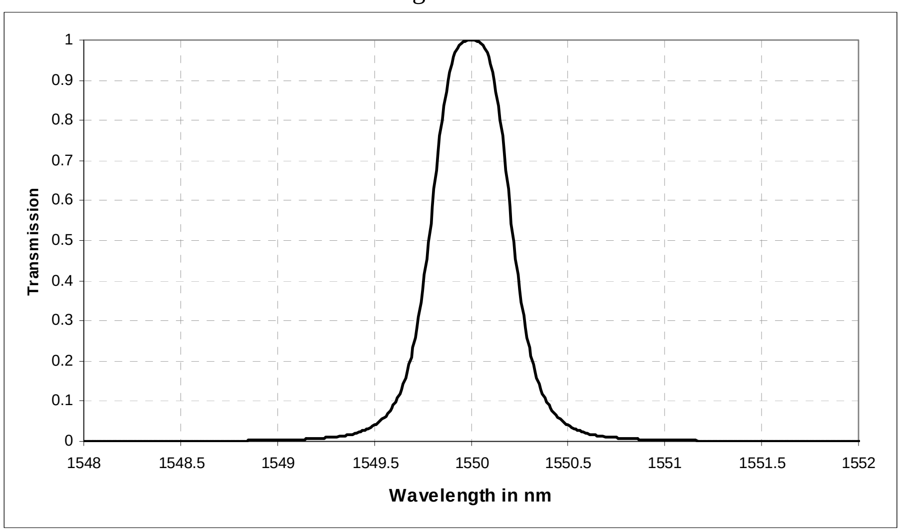

Fig. 2. Theoretical transmission of the double-cavity filter.

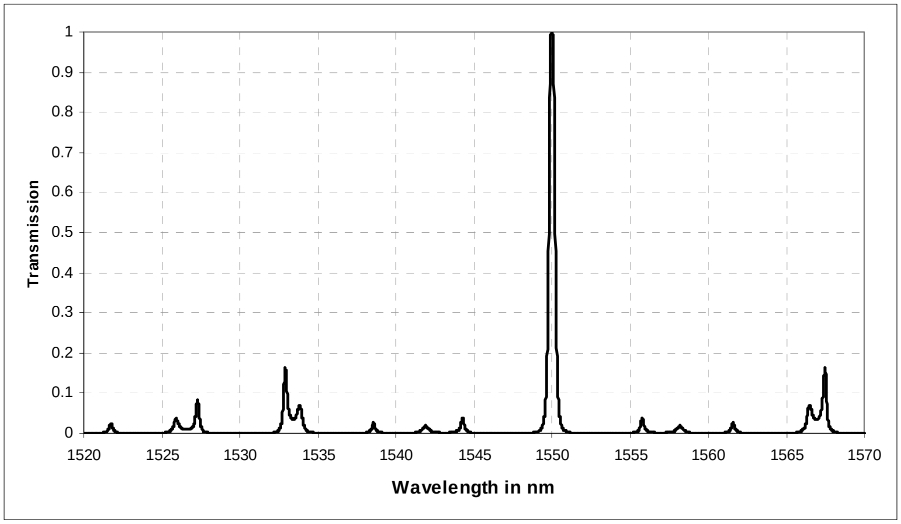

Fig. 3. Theoretical transmission of the double-cavity filter between 1520 and 1570nm.

3. Experimental demonstration

For the experimental demonstration, we use a 100µm-silica-substrate (1”-parallelism, thermal sensitivity 9pm/°C, extinction coefficient less than 10^{-6}) and a 60µm-silicon-substrate (3”-parallelism, thermal sensitivity 84pm/°C, extinction coefficient of $4.5.10^{-5}$). Their optical thicknesses are approximately the same as those mentioned in Section 2. The silica thickness is adjusted by a silica coating deposited by DIBS (Dual Ion Beam Sputtering) technology to insure the coincidence at 1550nm. 5-layer-SiO_2/Ta_2O_5 mirrors and 4-layer-SiO_2/Ta_2O_5 mirrors are deposited on both sides of each cavity by DIBS (with optical monitoring) according to Section 2. The setup used to measure the transmission makes use of a tunable laser source emitting in the C-band [1520-1570nm] with a wavelength repeatability of about 10pm. The laser beam is directed toward the filter with a monomode fiber ended by a pigtailed collimator. The beam waist (radius about 250µm) is located on the filter. The transmitted light is collected with an identical collimator and a monomode fiber which is connected to an InGaAs photodiode followed by a low noise current amplifier and a 16 bits digital to analog converter. The source and the measurements are computer controlled. The filter is placed in a thermo-regulated sample holder associated with an external Peltier thermoelectric controller (the stability of the temperature is better than 0.1°C). Our system needs several tens seconds for thermal stabilization. Moreover, tuning the temperature over several tens of degrees is time consuming. With theses considerations, the time interval between two spectral acquisitions at different temperatures is fixed to approximately 5 minutes.

Figure 4 represents the experimental transmission spectra of both filters at 25°C. The transmission maximum is near 100% for the silica filter and is about 87% for the silicon filter.

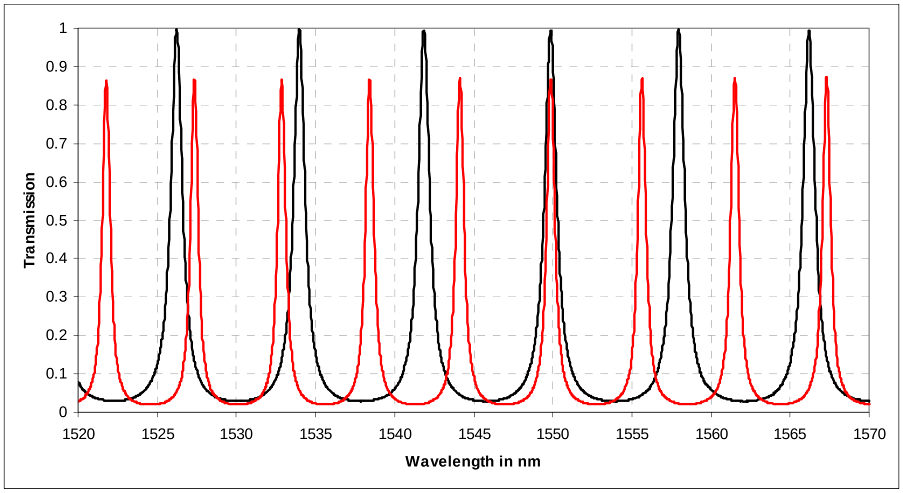

Fig. 4. Experimental transmission of both filters at 25°C (black: silica filter; red: silicon filter).

The thermal dependence of each filter has been measured between 25°C and 80°C. The behaviour is perfectly linear in both cases, with a slope of 9 pm/°C for the silica filter and 84pm/°C for the silicon filter, slightly smaller than the expected ones. Moreover, no hysteresis effects are observed and the thermal stability of the filters is ensured since we use hard and very stable DIBS coatings. A temperature higher than 350°C typically is required to induce irreversible measurable opto-geometrical parameter variations of the coatings.

The next step consists in assembling both filters in order to obtain the double-cavity structure. Numerical calculations show that the residual air gap thickness between both filters should be adjusted to a quarter-wavelength thickness with an 80nm-tolerance. This precision is achieved by trial and error. The procedure consists in holding both filters tight, trying several applied strengths. Such structures should be improved by using optical contacting technique [15,16]. Promising results with passive multiple-cavity filters have been yet obtained [17]. Figure 5 shows the measured transmission window of the double-cavity filter (at 25°C). Figure 6 is a movie that shows the transmission changes of this double-cavity filter when the temperature is progressively increased.

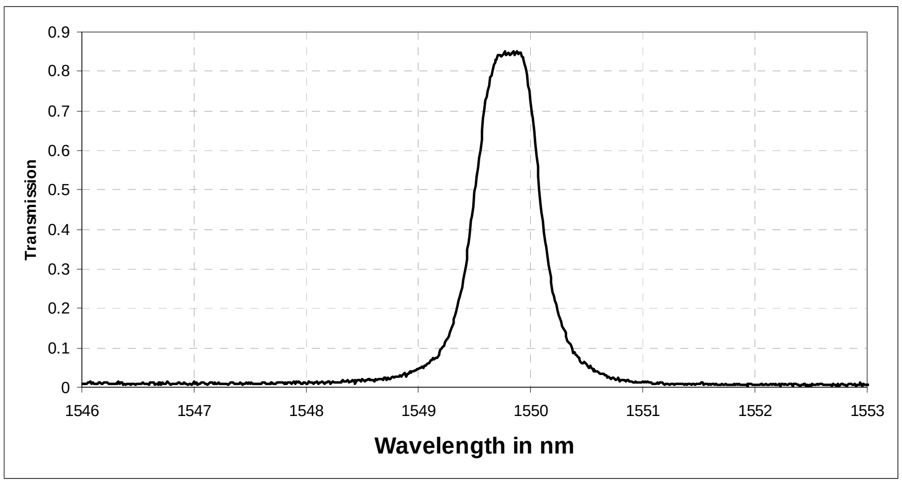

Fig. 5. Experimental transmission of the double-cavity filter.

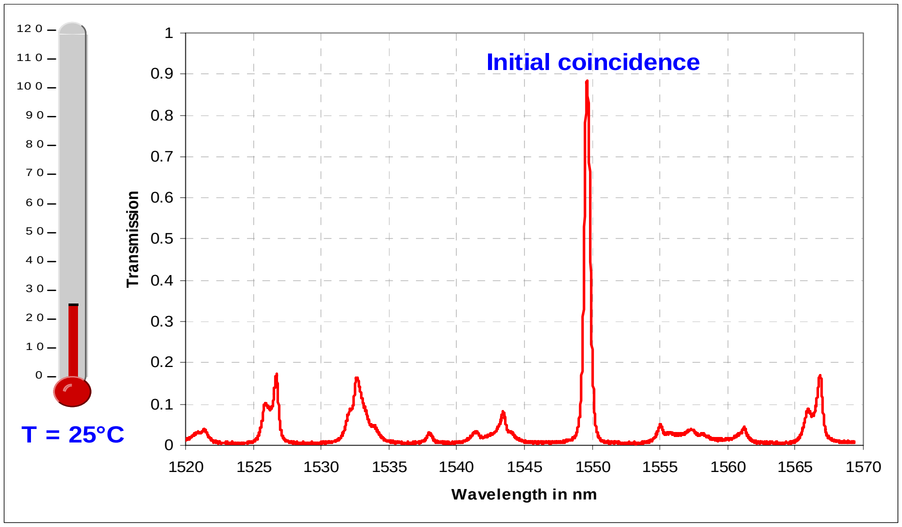

Fig. 6. (582 KB) Movie of the successive experimental coincidences for the double-cavity filter.

Table 2 gives experimental results in a similar way as table 1. The initial coincidence occurs at T=25°C.

Table 2: Experimental coincidences and related sensitivities

ΔT (°C)	*Center wavelength (nm)*	*Spectral shift (nm)*	*Differential sensitivity (pm/°C)*
0	1549.85	0	
12	1533.82	-16.0	-1420
31	1558.04	24.2	+1361
43	1542.10	-16.2	-1411
53	1526.27	-15.8	-1403

Further coincidences could not been achieved because our experimental apparatus is limited to a maximal temperature of 80°C. The experimental values of the required temperatures changes are slightly different from those given by the theory. The average differential sensitivity (1399pm/°C) is 20% higher than the expected one. For each coincidence, the transmission maximum is above 85%.

4. General method of synthesis

In a more general approach, we can demonstrate that it is possible to calculate all the triplets (d_1, d_2, ΔT), where d_1 and d_2 are the cavity thicknesses and ΔT is the applied temperature variation, permitting the filter to switch from a given channel of the 100 GHz ITU grid (number *p*) to another one (number *p*+*q*) into the C-Band (1530 – 1570nm). For simplicity, we concentrate on double-cavity tunable filters with cavities in silica and silicon.

The main milestones of this design method are as follows. We suppose first that the initial coincidence is at λ_0 = 1550nm. Then, we have:

$$\lambda_0 = \frac{2n_1(\lambda_0)d_1}{k_0} = \frac{2n_2(\lambda_0)d_2}{m_0} \qquad (2)$$

where k_0 and m_0 are integers. Equation (2) defines the initial set of all the possible cavity thicknesses. From a practical point of view, we consider cavity-thicknesses comprised between 50 and 150µm for silica ($90 < k_0 < 300$) and between 50 and 90µm for silicon ($200 < m_0 < 400$).

The transmission of each filter is maximal for the wavelengths respectively defined by:

$$\lambda_k = \frac{2n_1(\lambda_k)d_1}{k_0 + k} \quad \text{and} \quad \lambda_m = \frac{2n_2(\lambda_m)d_2}{m_0 + m} \tag{3}$$

where $n_1(\lambda_k)d_1$ and $n_2(\lambda_m)d_2$ are the optical thicknesses of the silica and silicon cavities (at the wavelengths λ_k and λ_m), k and m are relative integers whose absolute value is typically less than 10 ($m << m_0$ and $k << k_0$). Here, we have taken into account the chromatic dispersion of the materials of both cavities. The dispersion laws are those of fused silica and bulk silicon [12]. A temperature variation ΔT applied on the 2-cavity filter induces a spectral shift of both λ_k and λ_m. Then, the new wavelengths of maximal transmission are:

$$\lambda_k^T = \lambda_k\left[1 + \beta_1 \Delta T\right] \quad \text{and} \quad \lambda_m^T = \lambda_m\left[1 + \beta_2 \Delta T\right] \tag{4}$$

where β_1 and β_2 are the thermal sensitivities of silica and silicon. The new coincidence is supposed to be λ_p. Then, by using the relationship $\lambda_k^T = \lambda_p$, we obtain:

$$\Delta T = \frac{1}{\beta_1}\left[\left\{\frac{n_1(\lambda_0)\lambda_p}{n_1(\lambda_k)\lambda_0} - 1\right\} + \frac{k\lambda_p}{2n_1(\lambda_k)d_1}\right] \tag{5}$$

In the C-Band, the dispersion laws of the cavities can be approximated by a linear relationship. Thus, we can write:

$$n_1(\lambda_k) = n_1(\lambda_0) + (\lambda_k - \lambda_0)\frac{\partial n_1}{\partial \lambda} \tag{6}$$

By injecting Eq. (6) into Eq. (5), we obtain, in this first order approximation, the following expression for the temperature variation:

$$\Delta T = \frac{1}{\beta_1}\left[\frac{k}{k_0\lambda_0}\left\{\lambda_p + \frac{\lambda_0^2}{n_1(\lambda_0)}\frac{\partial n_1}{\partial \lambda}\right\} + \frac{\lambda_p}{\lambda_0} - 1\right] \tag{7}$$

Equation (7) can be used to calculate, for a given k and a given d_1 (defined by Eq. (2)), all the temperature variations ΔT enabling the switch from the channel λ_0 to the channel λ_p. A similar equation is obtained for the silicon cavity. Thus, we obtain a first table of [k_0, k, ΔT] values for the silica cavity and a second table of [m_0, m, ΔT'] for the silicon one. In order to achieve a switch of the double cavity-filter from channel λ_0 to channel λ_p, we must select only the solutions which correspond to the same temperature variation (ΔT = ΔT'). In general, several solutions exist. The selection of the optimal configuration is then made by considering first the gain in sensitivity, i.e., the ratio between the temperature variation needed to achieve the same spectral shift for the single silicon cavity and this ΔT value. Moreover, rejection level outside the passband and spectral bandwidth are to be considered. These both last properties can be improved by increasing the number of cavities and/or the number of mirror-layers. It can be noted that this approach can be identically applied whatever the number and the nature of the cavities we consider.

As an example, we show on Fig. 7 the transmission of a filter corresponding to an 8-channel switching. The thicknesses of the cavities are 133.10µm for silica (k_0 = 248) and 63.74µm for silicon (m_0 = 286). The temperature variation ΔT is 15°C and the involved interference order variations are k = -1 and m = -1 respectively. The black curve shows the filter in its initial position on the channel 501 of the general ITU grid (central wavelength 1550.12nm). The red curve shows the filter positioned on the channel 565, i.e., 8 channels away on a 100 GHz grid (central wavelength 1556.55nm). The resulting sensitivity is 418pm/°C. The vernier effect introduces a gain of 5 with respect to the intrinsic sensitivity of silicon.

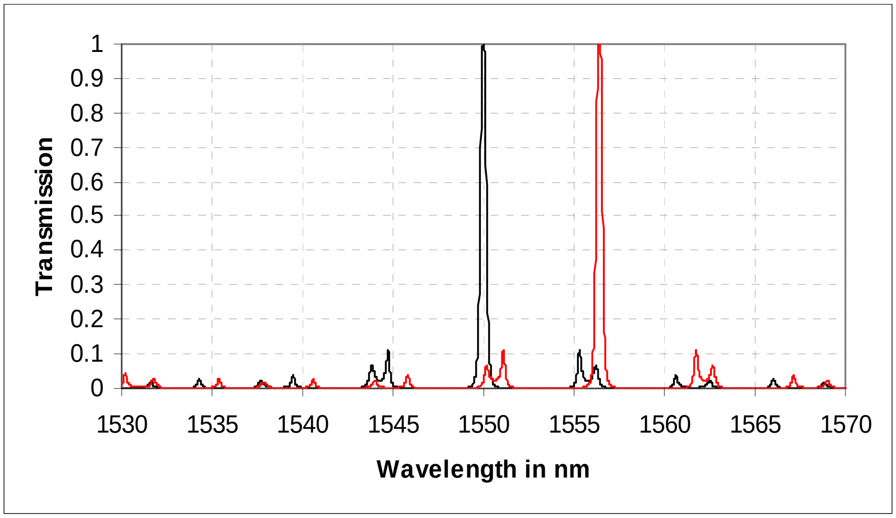

Fig. 7. Eight-channel tunability (black: initial coincidence; red: final coincidence).

Another example is for a 16-channel switching. The cavity thicknesses are 67.09µm for silica (k_0 = 125) and 35.88µm for silicon (m_0 = 161). The temperature variation is 40°C (gain by a factor about 3) and the involved interference order shifts are also k = -1 and m = -1 respectively. It has to be noted that we considered in this case 7-layer mirrors for the silica-cavity filter. The Fig. 8 represents the transmission of the filter. As for the Fig. 7, the black curve shows the filter in its initial position (channel 501; 1550.12nm) and the red curve shows the filter positioned 16 channels away (channel 630; 1563.05nm).

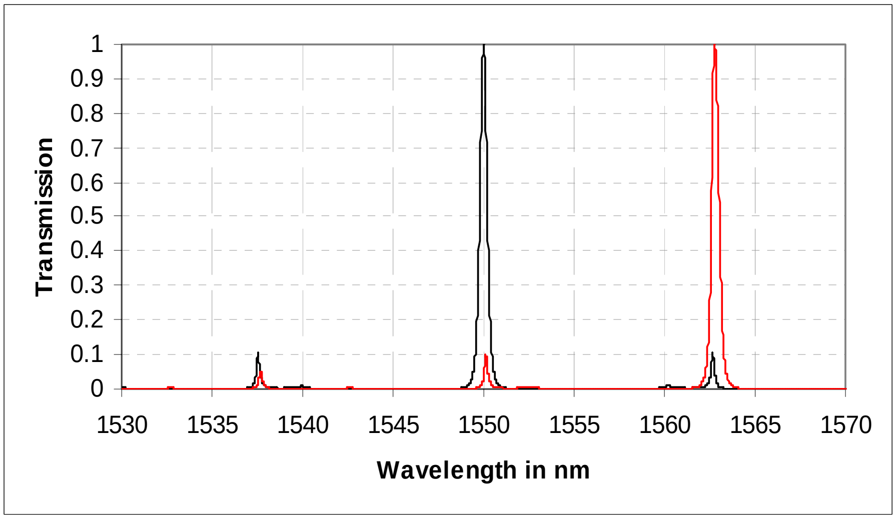

Fig. 8. Sixteen-channel tunability (black: initial coincidence; red: final coincidence).

5. Conclusion

In this paper, we demonstrated that contacted double-cavity solid-spaced bandpass filters are an efficient solution to achieve filters which can be tuned over the optical telecommunications C-Band with moderate temperature changes. An increase of sensitivity by a factor about 10 is possible for a double-cavity silica/silicon filter. The spectral features of the resulting filter are pseudo-periodic with the temperature. The results of our experimental demonstration are in good agreement with the theoretical predictions.

Optical contacting is the right way to assemble these two filters in a compact and resistant item. Additional studies concerning the long-term stability of the component (thermal cycling, aging) and its dynamic behaviour (response time) should be performed to ensure the viability of such filters in an industrial context.